Climate Dynamics (2002) 18: 647–660
DOI 10.1007/s00382-001-0193-9

B. Delmonte · J.R. Petit · V. Maggi

Glacial to Holocene implications of the new 27000-year dust record from the EPICA Dome C (East Antarctica) ice core

Received: 4 January 2001 / Accepted: 7 July 2001 / Published online: 23 March 2002

Abstract Insoluble dust concentrations and volume-size distributions have been measured for the new 581 m deep Dome C-EPICA ice core (Antarctica). Over the 27000 years spanned by the record, microparticle measurements from 169 levels, to date, confirm evidence of the drastic decrease in bulk concentration from the Last Glacial Maximum (LGM) to the Holocene (interglacial) by a factor of more than 50 in absolute value and of about 26 in flux. Unique new features revealed by the EPICA profile include a higher dust concentration during the Antarctic Cold Reversal phase (ACR) by a factor of 2 with respect to the Holocene average. This event is followed by a well-marked minimum that appears to be concomitant with the methane peak that marks the end of the Younger Dryas in the Northern Hemisphere. Particle volume-size distributions show a mode close to 2 μm in diameter, with a slight increase from the LGM to the Holocene; the LGM/Holocene concentration ratio appears to be dependent on particle size and for diameters from 2 to 5 μm it changes from 50 to 6. Glacial samples are characterised by well-sorted particles and very uniform distributions, while the interglacial samples display a high degree of variability and dispersion. This suggests that different modes of transport prevailed during the two climatic periods with easier penetration of air masses into Antarctica in the Holocene than during Glacial times. Assuming that southern South America remained the main dust source for East Antarctica over the time period studied, the higher dust content recorded during the ACR which preceded the Younger Dryas period, represents evidence of a change in South America environmental conditions at this time. A wet period and likely mild climate in South America is suggested at circa 11.5–11.7 kyr BP corresponding to the end of the Younger Dryas. The Holocene part of the profile also shows a slight general decrease in concentration, but with increasingly large particles that may reflect gradual changes at the source.

B. Delmonte (✉) · J. R. Petit
Laboratoire de Glaciologie et de
Géophysique de l'Environnement,
BP96, 38402, Saint Martin d'Hères, France
E-mail: bdelmonte@nest.it

B. Delmonte · V. Maggi
University of Milano-Bicocca,
Dipartimento Scienze Ambientali,
Piazza della Scienza 1, 20126 Milano, Italy

1 Introduction

Records of insoluble microparticles (dust) in ice cores provide one of the most detailed and best preserved sources of paleoclimatic information, in particular in terms of past storminess and dustiness as well as the location, extent and conditions of source areas (Svensson 1998). Dust data are useful for the reconstruction of past circulation patterns and environmental conditions using general climate models (GCM). The role of mineral aerosol in the climate dynamics is quite complex and not yet fully understood, but exerts a radiative forcing effect on the climatic system (Sokolik and Toon 1996). Dust may also contribute to biogeochemical cycles (Kumar and Anderson 1995; De Baar et al. 1995) and therefore participate in atmospheric CO_2 regulation.

There is considerable evidence in paleoenvironmental archives from polar and low-latitude ice cores (e.g. De Angelis et al. 1987; Hansson 1994; Thompson et al. 1995; Steffensen 1997; Petit et al. 1981, 1999; Briat et al. 1982) and from marine (e.g. Rea 1994) and terrestrial deposits (e.g. Kukla 1989) that the atmospheric dust load, and consequently deposition in oceans and on continents, was greater during glacial periods. A recent estimate suggests a 2.5 fold increase of the mean value on a global scale (Mahowald et al. 1999) during the last glacial maximum (LGM). However, the increase is much greater for polar latitudes and Antarctic ice cores from Dome C and Vostok have revealed an LGM flux 10 to

20 times greater than that of the Holocene (Petit et al. 1981, 1990; De Angelis et al. 1984). Similarly, for the GRIP ice core (Summit, Greenland), the ratio between the highest peaks of the LGM and those of the current climatic stage yields an extreme value of about 68 (Steffensen 1997).

The high glacial dust input in East Antarctica can be explained by the synergetic action of many factors involving the atmosphere, biosphere, hydrosphere and lithosphere. There are three basic conditions to consider: (1) the increased aridity on the continents due to changes in soil moisture and/or vegetation cover coupled with an enlargement of the dust-source areas caused by sea-level lowering (Petit et al. 1981; Joussaume 1990); (2) the more vigorous atmospheric circulation enhanced by the steeper southern temperature gradient generated by the northward extension of sea ice (COHMAP Members 1988) and (3) the reduction in the intensity of the hydrological cycle leading to less efficient scavenging by precipitation and consequently more efficient transport of dust (Joussaume 1989; Hansson 1994; Yung et al. 1996). Even when taking into account most of these factors, initial GCM simulations failed to reproduce the LGM dust increase for polar areas. Mahowald et al. (1999), however, recently obtained a 20-fold increase for high-latitude sites by adding a simulation of vegetation changes to a GCM. Vegetation traps dust and this effect is drastically reduced under glacial conditions.

Here we present the record of continental insoluble microparticles from the upper 581 m of a new ice core recovered during the 1997/98 and 1998/99 field seasons in the East Antarctic plateau at the Dome C site (75° 06' S, 123° 24' E). This ice core was drilled within the framework of the European Project for Ice Coring in Antarctica (EPICA). The elevation (3233 m) and the geographical location of the site make it suitable for paleoclimatic studies. Given the high altitude of the interior of the East Antarctic plateau, the site makes it possible to record the atmospheric aerosol background. For the dust emitted by the continental regions of the Southern Hemisphere (see Fig. 1), the small-sized component is transported over long distances to the polar area. This reflects a large-scale phenomenon including environmental changes in the source area associated with climate. Since the dust deposited in the East Antarctic ice cores during the glacial climate likely originated from Patagonia and South America (Grousset et al. 1992; Basile et al. 1997), the EPICA dust record can potentially provide information on the dynamics of the climate and environmental change of this area.

The EPICA core climatic record is deduced from the isotopic composition of the ice and the profile has been described in Jouzel et al. (2001). The chronology of the core (Schwander et al. 2001) has been established through an ice flow model coupled with temporal markers. These include the depths marked by volcanic events from the Vostok core dated over the last 7000 years (indirectly through comparison of ^{10}Be and ^{14}C production), the end of the Younger Dryas at 11.5 kyr BP taken from Greenland ice layer counting and matched to the EPICA core with the global CH_4 event, and the estimated depth of the ^{10}Be peak at 41 kyr BP. The time period covered by the core spans about 27000 years with an error of 0.25 kyr at 11.5 kyr BP and 1 kyr at 41 kyr BP (Schwander et al. 2001). The climatic record shows three main periods: the Holocene, characterized by high deuterium values, the isotopic transition, and the stage with minimum deuterium values corresponding to the Last Glacial Maximum and the end of the last glacial period. Taking the EPICA record as a climatic reference, Jouzel et al. (2001) compared and synchronised other isotopic records from Vostok, Dome B, Komsomolskaya and old Dome C cores. This provides a remarkable overview of the climate history of the East Antarctic plateau back to the LGM period. Interestingly, all the records clearly confirm the evidence of a two-step pattern of the last deglaciation. After an initial warming, a well-marked phase of cooling followed, referred to as the Antarctic Cold Reversal (ACR). The ACR preceded the cooling phase of Younger Dryas from the Northern Hemisphere by about 1 kyr (Jouzel et al. 1995). The Younger Dryas was characterised by a return to almost glacial climatic conditions with high dust content in Greenland ice, while the dust content from Antarctic record looks different during the ACR, reaching a level close to the Holocene value (Jouzel et al. 1995).

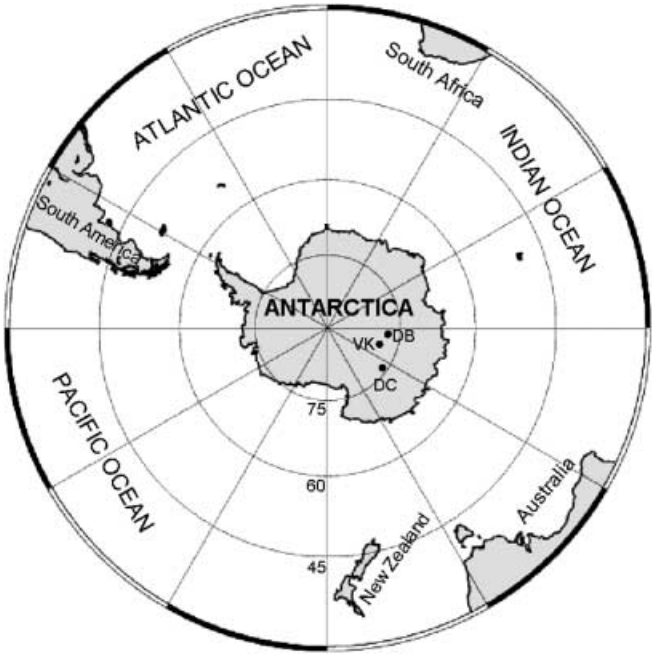

Fig. 1. Map of the Southern Hemisphere with the main locations discussed in this paper. *DC*: Dome C; *DB*: Dome B; *VK*: Vostok

Taking advantage of the good quality of the EPICA ice core and some improvements in laboratory dust measurements, we will document this mid-deglaciation and the other periods. We will also characterise the size distributions of the dust particles over the entire length

of the record and discuss the variations in terms of changes in transport and/or environmental changes over the sources. We will finally compare this Antarctic record with Greenland dust records.

2 Analytical procedure

A total of 169 ice increments taken from depths of 10 m to 581 m were analysed. Each 5-cm long sample represents about 2 years for the Holocene and 4 to 5 years for the LGM period, because of some thinning of the ice, as well as the halving of snow accumulation rate between the two periods (Jouzel et al. 1987, 2001). The mean resolution is one sample per 3 to 4 m of ice (i.e. one sample per about 135 years) for the Holocene period and one sample per 2 to 3 m (about 230 years) for the LGM.

Ice samples were decontaminated by three repeated washings in ultra-pure water (MilliQ). For the porous firn, the outer part of the samples was scraped away over about 2 mm of thickness using a lathe. For the firn part down to 100 m depth, we selected one ice core increment every 5 m and analysed several 5-cm long adjacent sub-samples to check our decontamination procedure. Data for the uppermost 40 m of the core (spanning the last 700 yrs) are not reported here since the use of the lathe, the very high porosity of the firn and the low number of available measurements do not allow us to exclude the possibility of contamination of these samples.

The measurements of dust concentration and size distribution were performed using a Multisizer IIe©Coulter Counter set up in a class 100 clean room. The instrument works on the basis of the detection of the electric signal generated by the particles that are forced to flow through a small aperture tube (50 μm in diameter). The water sample is made conductive by adding a pre-filtered 20% NaCl electrolyte solution giving a 1% concentration to the final solution. Melted samples were mechanically stirred continuously before the analysis in order to prevent sedimentation in the container. At least three consecutive counts were performed on each volume of 500 μl. The reproducibility of the measurements is good for highly concentrated samples (better than 2% for 50000 particles per gramme), while some scattering may occur for samples with low concentrations (up to 20% for 1000 particles per gramme). The particle size is expressed by the diameter of a sphere with an equivalent volume. The mass was calculated from the measured volume assuming a particle density of 2.5 g/cm^3. The instrument was set for measurements of particles with diameters from 0.7 to 20 μm in 256 channels on a logarithmic scale. Similar techniques and procedures were used by Steffensen (1997) to perform measurements on the GRIP ice core.

Statistical analyses were performed on the volume-size distributions of particles along the core. All distributions were considered from 0.7 μm to the uppermost limit of the continuous distribution curve that is about 5 μm for the EPICA core. This makes it possible to separate spurious counts caused by electric noise and/or big particles due to possible contamination of the samples. This effect is significant for the Holocene samples with low concentrations. For example, more than 99% of the total counts are included in the interval from 0.7 to 5 μm for both LGM and Holocene samples, but the contribution of particles greater than 5 μm to the total volume may represent up to 2% and 40%, respectively.

The volume-size distributions of samples were fitted with a lognormal function, as suggested by several authors (Patterson and Gillette 1977; Royer et al. 1983, Steffensen 1997).

$$\mathrm{dV/d\,Ln\,D} = \mathrm{a}^{*}\exp[-0.5^{*}(\mathrm{Ln}\,(\mathrm{D/D_v})/(\mathrm{Ln}\sigma_\mathrm{g}))^2] \quad (1)$$

where

$$\mathrm{a} = \mathrm{V}/[(2\Pi)^{1/2*}\mathrm{Ln}\sigma_\mathrm{g}] \quad (2)$$

The distribution is defined by three parameters: the total volume V, the modal diameter D_v, where the derivative is null, and (σ_g) the geometric standard deviation which describes how closely the particle volume is distributed around the mean. This function is quite useful since the n-th moment of a lognormal function is also a lognormal function with the same σ_g but with a mean diameter $\mathrm{D_m}$ (Royer et al. 1983):

$$\mathrm{D_m} = \mathrm{D_v}^{*}\exp[\mathrm{n}^{*}(\mathrm{Ln}\sigma_\mathrm{g})^2] \quad (3)$$

Therefore, the modal diameter of the volume distribution (D_v) can be easily transformed to the corresponding number mean diameter D_n, while the geometric standard deviation σ_g is common to all the distributions.

The lognormal regressions provide a reasonable initial estimate of the dust distributions. However with our high-resolution measurements (256 channels) and for highly concentrated samples, some differences occur: the mode of the distribution is slightly shifted and the volume distribution appears slightly left-skewed (Fig. 3a). A better fit could be obtained using a four-parameter Weibull function (Fig. 3b).

$$\mathrm{dV/d\,Ln\,D} = \mathrm{a}^{*}((\mathrm{c}-1)/\mathrm{c})^{((1-\mathrm{c})/\mathrm{c})*}(\mathrm{g}^{(\mathrm{c}-1)})^{*} \times \exp(-\mathrm{g}^{\mathrm{c}}) + ((\mathrm{c}-1)/\mathrm{c}) \quad (4)$$

where

$$\mathrm{g} = \mathrm{abs}\,((\mathrm{D}-\mathrm{D_v})/\mathrm{b} + ((\mathrm{c}-1)/\mathrm{c})^{1/\mathrm{c}}) \quad (5)$$

This function provides a slightly improved correlation coefficient (Table 1).

3 Results

The profile of dust concentration in the EPICA core versus depth is shown in Fig. 2a, along with the deuterium record. The number of particles/ml and mass content (ppb) have been plotted on a logarithmic scale since it is assumed that dust concentration in snow is the end result of a series of phenomena and factors having a synergetic (multiplicative) effect. The average number and mass concentrations every 20 m are also shown in Table 1.

The EPICA dust record indicates a drastic decrease in continental windblown dust from the LGM (195000 particles/ml, 790$^{*}10^{-9}$ g*g^{-1} or 790 ppb for depth interval 480–580 m) to the warm Holocene period (3900 particles/ml, 15 ppb for depth interval 40–360 m). The ratio between mean LGM and Holocene concentrations is greater than 50 for both particle number and mass. As the snow accumulation rate changes by a factor of 2 between the two periods (Jouzel et al. 1987, 2001), a dust flux ratio of about 26 is inferred.

The same general behaviour can be found in the dust records of the other East Antarctic ice cores (Vostok, Dome B and old Dome C, Fig. 2) along with their respective isotopic profiles. For the three ice cores, the LGM to Holocene ratio is respectively 24, 35 and 28 (Table 2), which is lower than the ratios for our EPICA data. However, while the LGM concentrations are almost the same between the cores, their Holocene values are higher than the values for EPICA. Since the number of measurements was rather low for these cores and the analytical procedure less reliable than the one we used for EPICA, we cannot

Table 1. EPICA dust concentration (number and mass) along with the parameters for the lognormal (a normalised volume parameter, D_v mode diameter and σ_g geometric standard deviation) and Weibull regressions (parameters a, b, c) of volume-size distributions, averaged over every 20 m of depth. D_n represents the calculated mode of the number-size distribution (see text)

		Particle concentration													
		(Average every 20 m of depth)		Log-normal						Weibull					
Depth (m)	N.samples	Number/ml	Mass (p.p.b.)	correlation	a	Dv (um)	Standard error of Dv	Geometric standard deviation	Dn^{**} (um)	correlation	Dv (um)	Standard error of Dv	a	b	c
40-60	3	3027	9.5	0.87	0.95	2.03	0.03	1.98	0.50	0.87	2.14	0.05	0.94	2.85	1.59
60-80	4	3252	11.6	0.82	0.91	2.28	0.05	2.16	0.38	0.87	2.30	0.05	0.91	3.21	1.56
80-100	4	3929	14.9	0.88	0.97	2.04	0.03	1.92	0.57	0.87	2.15	0.04	0.96	2.76	1.62
100-120	5	2893	10.6	0.85	0.99	2.15	0.04	1.91	0.61	0.84	2.25	0.05	0.97	2.88	1.62
120-140	6	2923	10.8	0.91	1.01	2.15	0.03	1.85	0.69	0.92	2.33	0.04	1.01	2.74	1.84
140-160	5	3276	12.8	0.88	1.04	2.18	0.03	1.81	0.76	0.89	2.43	0.05	1.06	2.81	2.15
160-180	6	3151	11.3	0.88	0.97	2.14	0.03	1.94	0.57	0.87	2.24	0.05	0.95	2.98	1.57
180-200	5	3035	12.6	0.93	1.11	2.14	0.02	1.71	0.90	0.94	2.33	0.03	1.11	2.52	2.05
200-220	5	3071	16.5	0.90	1.10	2.05	0.03	1.72	0.85	0.92	2.24	0.04	1.11	2.41	2.02
220-240	6	4004	15.6	0.88	0.97	2.27	0.04	1.97	0.57	0.87	2.40	0.05	0.95	3.15	1.62
240-260	6	4456	16.8	0.96	1.12	1.92	0.01	1.69	0.84	0.96	2.05	0.02	1.10	2.19	1.85
260-280	5	4669	20.4	0.90	1.07	2.05	0.03	1.75	0.80	0.90	2.16	0.04	1.05	2.44	1.75
280-300	5	3737	14.1	0.91	1.03	2.00	0.02	1.82	0.68	0.90	2.08	0.04	1.00	2.52	1.63
300-320	5	4276	16.0	0.94	1.07	2.00	0.09	1.75	0.78	0.94	2.16	0.03	1.06	2.40	1.86
320-340	6	4071	14.2	0.95	1.06	1.91	0.02	1.76	0.73	0.96	2.07	0.02	1.05	2.33	1.84
340-360	5	5684	21.7	0.95	1.05	1.98	0.02	1.78	0.73	0.94	2.07	0.03	1.03	2.41	1.68
360-380	7	3478	11.3	0.91	1.03	1.86	0.02	1.81	0.65	0.91	1.93	0.04	1.01	2.31	1.62
380-400	8	6922	34.8	0.97	1.09	1.99	0.01	1.72	0.83	0.97	2.14	0.02	1.08	2.32	1.87
400-420	7	7762	29.0	0.97	1.08	1.91	0.01	1.74	0.76	0.97	2.01	0.02	1.06	2.25	1.72
420-440	7	9751	35.7	0.97	1.06	1.94	0.01	1.77	0.74	0.98	2.07	0.02	1.05	2.34	1.77
440-460	7	37958	120.8	0.99	1.15	1.71	0.01	1.67	0.78	1.00	1.79	0.01	1.12	1.89	1.75
460-480	7	105007	361.9	0.99	1.19	1.80	0.01	1.63	0.88	1.00	1.93	0.00	1.17	1.96	1.94
480-500	7	214440	850.7	0.99	1.21	1.90	0.01	1.61	0.97	1.00	2.06	0.00	1.20	2.06	2.06
500-520	7	180006	724.3	0.99	1.25	1.89	0.01	1.58	1.01	1.00	2.03	0.00	1.23	1.98	2.07
520-540	8	181232	716.3	0.98	1.21	1.90	0.01	1.61	0.97	1.00	2.05	0.00	1.20	2.05	2.04
540-560	7	185890	743.0	0.99	1.21	1.91	0.01	1.60	0.98	1.00	2.05	0.00	1.20	2.04	2.04
560-580	7	216022	862.4	0.98	1.24	1.95	0.01	1.59	1.03	1.00	2.11	0.00	1.23	2.08	2.12

exclude the possibility of contamination in their Holocene concentrations.

Based on the stable isotope content, the deglaciation occurs in two steps and a cold phase appears in the middle of deglaciation, corresponding to the ACR (420–375 m depth in the EPICA core, Fig. 2a). In this depth interval, the microparticle mass concentration is about 30 ppb and therefore twice as large as the mean Holocene concentration. Moreover, between 360 and 373 m depth, the dust record shows a well-marked period of extremely low dust concentrations, with a mean particle mass of 7 ppb and an absolute minimum of 2.9 ppb observed at 371 m depth.

From the onset of the Holocene to the uppermost part of the core, the EPICA dust profile suggests, over and above the natural variability of the data, a slight but significant general decrease with a rate of about 0.9 ppb per 1000 years in mass and 200 particles/ml per 1000 years in number. This tendency seems to be common to all records and particularly evident for the Vostok data, however this may be simply a coincidence (Fig. 2b).

In Fig. 3 we show the average volume-size distributions of all Holocene and LGM samples, normalised to 100% in the interval between 0.7 and 5 μm. A slight increase in the mode of the distribution (D_v) can be observed from LGM (1.91 ± 0.02 μm) to Holocene (2.08 ± 0.12 μm) samples, and simultaneously the values of σ_g increase. These two parameters were averaged every 20 m of depth and are displayed in Table 1 along with the calculated values for D_n. Note that the mean diameter of the size-number distributions is smaller for Holocene than for LGM particles, because of a greater value for σ_g (Fig. 3a). Sub-micron particles are, therefore, proportionally more numerous during the Holocene, but obviously this has little influence on the total mass.

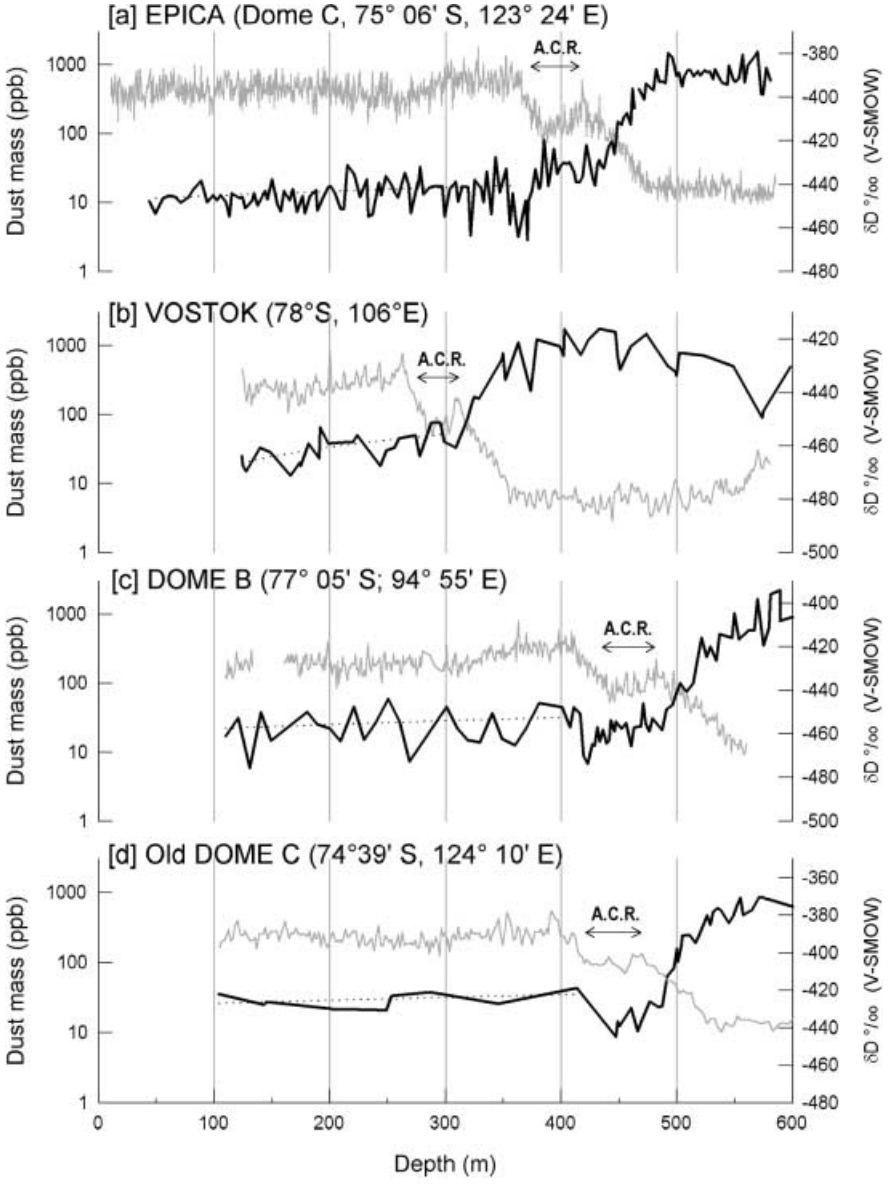

Fig. 2a–d. Record of insoluble dust mass (*black line*) and Deuterium (*grey line*) versus depth (Jouzel et al. 2001) for East Antarctica ice cores. From *top* to *bottom*: EPICA- Dome C (this work), Vostok (Petit et al. 1990), Dome B (Jouzel et al. 1995) and old Dome C (Royer et al. 1983). For the four cores, the Antarctic cold reversal phase of the isotope (ACR) is reported; the Holocene is on the left side of the profile while the glacial period is on the right. A slight decreasing trend for the particle mass during the Holocene is suggested in all profiles by the *dotted line*

Table 2. Average dust mass concentration for the Holocene and LGM in four East Antarctic ice cores and the approximate time frequency of sampling for the two climatic periods. The number of samples analysed for the Holocene is 81 for the EPICA core (this work), 24 for Vostok (Petit et al. 1990), 51 for Dome B (Jouzel et al. 1995), and 17 for old Dome C (Royer et al. 1983)

Ice core	Average Holocene dust mass (ppb)	Sampling frequency Holocene (yrs)	Average LGM dust mass (ppb)	Sampling Frequency L.G.M (yrs)	LGM/Holocene Abs. Concentration
EPICA	15 ± 7	135	790 ± 290	230	53
VOSTOK	35 ± 18	~600	849 ± 471	~600	24
DOME B	25 ± 12	~300	875 ± 541	~500	35
Old Dome C	23 ± 10	~900	640 ± 169	~450	28

From the mode and the geometric standard deviation of the lognormal distribution, we deduce that 68% of the total volume (mass) is included in the interval of size expressed by [$\exp(Ln\ D_v - Ln\ \sigma_g)$; $\exp(Ln\ D_v + Ln\ \sigma_g)$]. This gives an interval from 1.11 to 3.81 μm for Holocene samples and from 1.20 to 3.05 μm for LGM samples, respectively. The narrower interval of glacial samples relative to the Holocene suggests LGM dust particles more closely distributed around the mean diameter or better sorted.

The mean value for D_v calculated with the Weibull function is 2.14 ± 0.18 μm along the whole core and it shifts from 2.06 ± 0.03 μm in the LGM to 2.21 ± 0.14 μm during the Holocene. While the absolute value of D_v is slightly different from the lognormal fit, the LGM-Holocene shift by ~ 0.15 μm is confirmed.

The records of the number and mass concentration along with the two parameters of the lognormal fit are shown in Fig. 4 against age. Number and mass concentrations (Fig. 4b, c) show a very similar pattern and two concentration peaks of 1470 and 1525 ppb occur in the glacial period at 19 and 26 kyr BP, respectively. Along the core, the data appears to be less scattered during the LGM than during the Holocene, even taking into account the smoothing effect that may be induced by the longer periods covered by each sample for the LGM than for the Holocene.

The large deglacial fall of both dust number and mass concentration starts at about 18 kyr BP (Fig. 4b, c) almost in concomitance with the beginning of the isotope rise and climate warming. The Holocene dust value reaches a first minimum at about 14.6 kyr BP, while the isotope rise instead continues until about 14 kyr. Then, the temperature decreases during the ACR phase and dust slightly increases again reaching concentrations two times higher than the mean Holocene level both in number and mass. After this, a second deglaciation step occurs and the dust concentration drastically drops to very low levels with a well-marked minimum at around 11.5–11.7 kyr BP (371 m depth) before reaching Holocene value. Then, the Holocene is characterised by a general decrease in mineral aerosol as already noted.

The modal values (D_v) and σ_g of the volume-size distributions are given in Fig. 4d, e along with average values over 20 m. The mean values along the entire core are 2.00 ± 0.13 μm and 1.78 respectively, but both

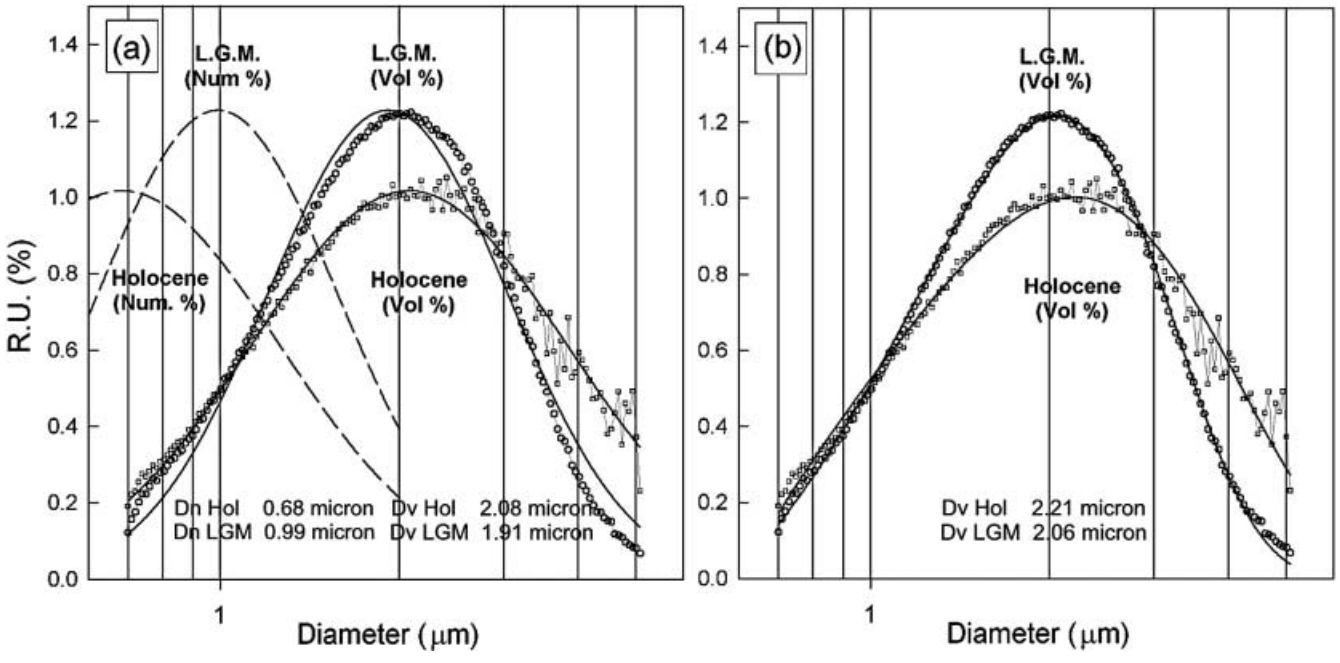

Fig. 3. **a** Lognormal and **b** Weibull regressions of Holocene and LGM average volume (mass)-size distributions expressed in relative units % (RU%). *Dashed lines* represent the calculated lognormal number-size distribution for the two climatic stages

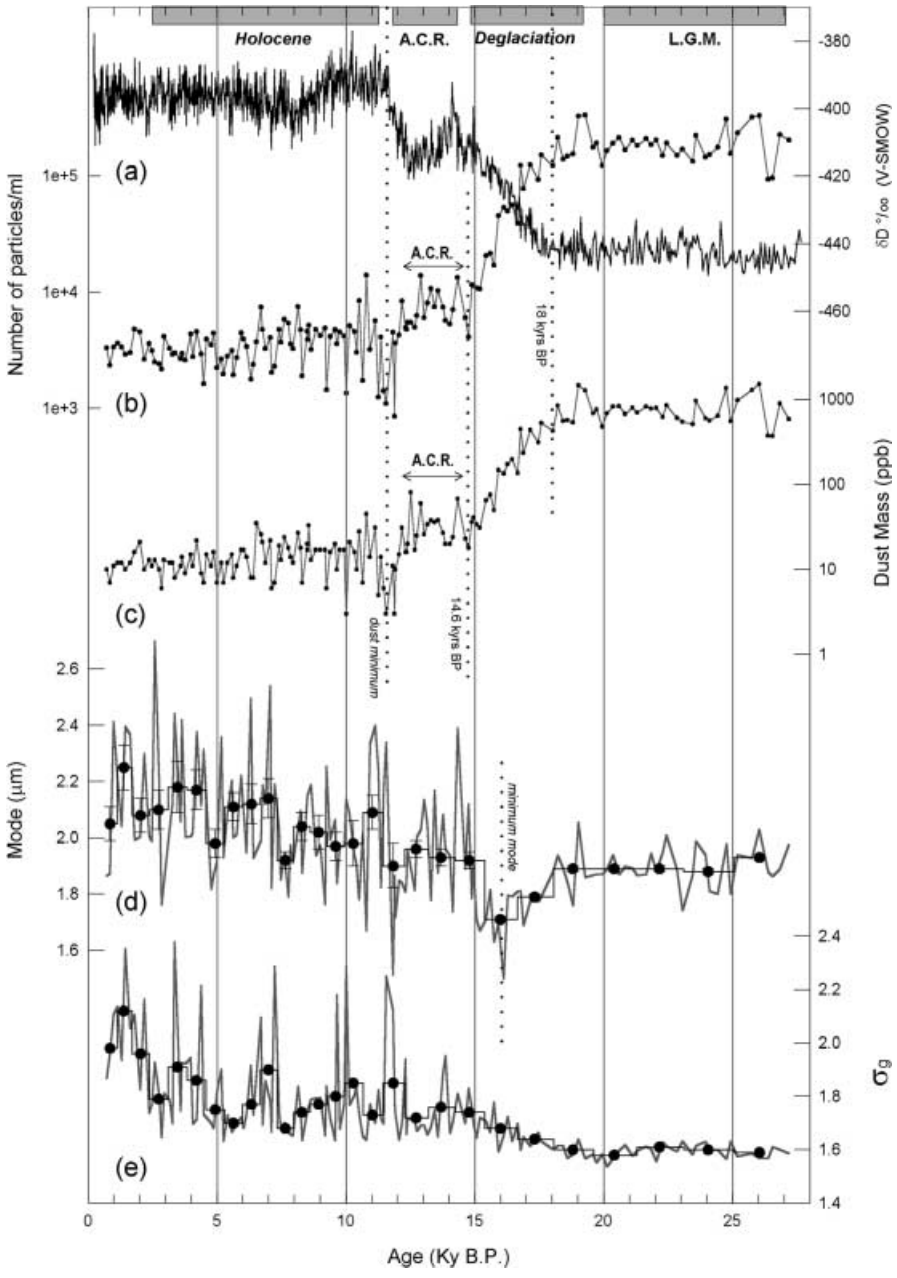

Fig. 4. EPICA dust number content **b**, mass concentration **c**, modal diameter **d** and geometric standard deviation **e** along with the deuterium profile **a** taken from Jouzel et al. (2001) and plotted versus age (from Schwander et al. 2001). The average values over 20 m are also plotted both for modal diameter (*black points* with error bars in **d**) and the geometric standard deviation (*black points* in **e**). The *grey areas* at the *top* represent, for each climatic period, the interval taken for characterisation of the insoluble particle distribution and displayed in Table 3a

parameters clearly show an increase from the LGM to the Holocene. Particles from the glacial period are characterised by low values for mode (1.91 ± 0.02 µm) and σ_g (1.6 ± 0.01), indicating fine and very well-sorted particles. Both parameters are almost constant over this climatic period. Note that at the start of the deglaciation, the onset of the dust decrease is concomitant with the uppermost limit of the narrow and well-sorted distributions of the glacial period. During the deglaciation, while σ_g increases regularly, the particle mode reaches a minimum at mid-deglaciation with average values of 1.7µm or even lower for individual samples. The Holocene particles display a highly variable character and coarser modes (2.08 ± 0.12 µm) and σ_g (1.8 ± 0.11). For both the parameters, the value progressively increases during the Holocene, and maximum values occur between 2 and 7 kyr BP. The change of the modal diameter along the EPICA core is independent on the type of regression chosen and same trend is confirmed when the Weibull fit is applied to the whole set of distribution data (Table 1). Only the absolute value of the mode is systematically shifted.

4 Discussion

4.1 Regional to inter-hemispheric significance of the EPICA dust record

The EPICA dust record shows an LGM/Holocene flux ratio of about 26. This change appears slightly higher than a previous estimate of 15 from the Vostok and old

Dome C cores (Petit et al. 1990), likely because of our lower EPICA concentration for the Holocene sample, while glacial concentrations remain similar to previous values. It also confirms that the drastic drop in dust concentration from glacial to Holocene levels occurs at about 14.6 kyr BP, according to the EPICA chronology. This level is an interesting temporal marker for Antarctic ice core records, assuming the dust source is the same for the different sites or governed by the same processes. Interestingly, Jouzel et al. (1995) assigned 14.6 kyr BP to the onset of Holocene dust levels in Antarctic cores based on several arguments such as the cross-check between Greenland and Antarctica methane and isotope composition from atmospheric oxygen entrapped in air bubbles, as well as the comparison with deep ocean core records. However before drawing conclusions on the representativeness of the dust records from East Antarctica, the question of the geographical origin of the source needs to be addressed.

Dust in Antarctic ice is mainly of continental origin (Briat et al. 1982; Gaudichet et al. 1988), as shown by the presence of various detrital minerals such as illite, crystalline silica, feldspar and smectite as well as volcanic glass shards (Gaudichet et al. 1986, 1988, 1992). Mineral dust reaching the interior of Antarctica is advected through the troposphere at levels higher than 4 km, the elevation of the East Antarctic plateau, after transport over very long distances. A contribution from nearby ice-free areas of Antarctica seems unlikely since it would be impeded by the katabatic winds blowing off the continent. Moreover, the surrounding cold ocean provides unfavourable conditions for atmospheric convection and the vertical ascent of particles. Isotopic fingerprints of glacial dust from Vostok and Dome C cores, based on $^{87}Sr/^{86}Sr$ and $^{143}Nd/^{144}Nd$ (Grousset et al. 1992; Basile et al. 1997) suggest that the Patagonia region of South America is the main source. The isotopic composition of loess and soils from this region closely matches the signature of ice core dust, to a far greater extent than any other potential source area or mixture of sources. This holds also for dust in interglacial ice for which preliminary measurements of the isotopic signature is compatible with a South American origin. (Basile 1997). The preferential atmospheric pathway for transport of dust from South America to East Antarctica is also suggested by the relative abundance of volcanic ash layers found in the Vostok core, originating from South Sandwich volcanoes in the southern South Atlantic (Basile 1997, Basile et al. 2001).

The Patagonian region was much colder and dryer during the LGM and fluvioglacial erosion processes were intense, forming an environment favouring dust mobilisation and deflation. There is evidence of a dry and windy climate over wide areas of South America during the late Quaternary period, including aeolian features, loess deposits, paleodunes and deflation basins (Clapperton 1993).

Furthermore, the glacial climate of South America was greatly influenced by the large extension of sea ice in the South Atlantic Ocean (Heusser 1989a). At the LGM, the polar front was displaced northward and consequently also the Westerlies belt. Compared to present-day, the spring limits of sea ice in the Southern Ocean during the last glacial period were about 3° to 5° latitude further north in the Pacific sector, 4° to 5° latitude further north in the Indian sector and at least 8° further north in the Atlantic (Burkle and Cirilli 1987). Therefore, sea-ice extent in the vicinity of South America, with the incipient closure of Drake Passage, presumably had an important influence in the climate of this region (Heusser 1989b). Similarly on the basis of glaciological data from Patagonia, Hulton et al. (1994) proposed that the LGM precipitation belt in South America shifted northwards by about 5° latitude with respect to the Holocene, located around 50°S. They suggested an LGM reduction of precipitation at 50°S as well as a lowering of the equilibrium line of the Southern Patagonian ice cap by 360 m at 56°S with respect to that of the Holocene.

The decrease in the dust concentration by an order of magnitude at the time of deglaciation is likely the result of concomitant factors. We believe that it is primarily linked to the changes in the Southern Ocean and a key role has been played by reduction of sea-ice extent in the Southern Atlantic Ocean, as supported by the drastic decrease in the sea-ice related diatom *E.Antarctica* (Burkle and Cooke 1983). This event likely occurred at the same time as the re-initiation of North Atlantic Deep Water formation (Charles and Fairbanks 1992). Given that the extent of sea ice and the intensity of the Westerlies are closely correlated (Simmonds 1981), the decrease of the polar front activity contributed to a reduction in the dust deflation at the source and the harsh environment over South America. The source area was also reduced by the melt water pulse (MWP1a, Fairbanks 1989), which likely submerged more than a half of the previously exposed continental shelf of Argentina (Jouzel et al. 1995). The onset of warmer climate made conditions less favourable for dust mobilisation and long-range transport: the southward shift of the precipitation belt (Lamy et al. 1999) led to a damp environment favouring a greater vegetation coverage as shown by paleo-vegetation proxies (Heusser 1989b). Moreover, greater evaporation and precipitation enhanced the hydrological cycle and led to more efficient scavenging of the aerosol. These factors could account for the drastic reduction of dust after the glacial period.

The general decreasing trend from $\sim$ 11 kyr BP to present may be the result of long-term changes to certain factors. The trend is very slight and gradual and rapidly changing sensitive features, such as vegetation cover or atmospheric circulation, are therefore probably not the main controlling factors. More likely, the trend is a combined result of a gradual reduction in the dust reservoir available for wind deflation by the reduction of glacier and periglacial processes, the progressive increase in biological activity and the development of pedogenesis.

The change in the paleoenvironment of the source regions is important as far as the dust cycle is concerned. The absolute minimum of the dust concentration is of particular interest in this respect. The EPICA profile shows a slight dust increase during the ACR phase and a well-marked minimum centred around 11.5–11.7 kyr BP. The latter corresponds to the end of the Younger Dryas in the Northern Hemisphere (11.5 ± 0.2 kyr BP), marked by a peak in methane concentration (Chappellaz et al. 1993). The methane event was associated with a sudden warming and an increase in biological (microbial) activity linked to the extension of wetlands in the Northern Hemisphere. East Antarctic records suggest that South American dust sources were also reduced probably because of a period of increased humidity. In this respect, McCulloch et al. (2000) suggest, on the basis of pollen records, a very wet phase in southern South America at the time of the last termination. Beside the higher precipitation linked to climatic changes, this region received an additional input of water derived from local sources such as Andean glaciers, snowcaps and permafrost, in response to probable local warmer conditions. This event may be therefore of a inter-hemispheric to global extent.

4.2 The Antarctic cold reversal (ACR)

The climate and environmental changes that occurred during deglaciation and the ACR phase are today of great interest. This mid-deglaciation cold episode is clearly evident in the isotopic record of deep Antarctic ice cores. On the other hand, the development of an event similar to the Younger Dryas (YD) at high latitudes on Southern Hemisphere continents, especially South America, is a matter of debate.

Wenzens (1999) reports a list of nine glacier advances which may have occurred in southern Patagonia (from 48°S to 51°S) at the time of the European YD. McCulloch and Bentley (1998) describe a glacial advance along the Strait of Magellan that they believe took place about 1 kyr earlier than the onset of the YD. Jouzel et al. (1995) has also concluded that the coldest part of the ACR preceded the YD by about 1 kyr. Evidence of a late-glacial re-advance has also been detected by Clapperton et al. (1995) for the central Magellan Strait, by Marden and Clapperton (1995 for Grey and Tyndall glaciers (51°08' and 51°15'S), and by Denton et al. (1999) for the southern Chilean lake district and from a proglacial lake in the nearby Argentine Andes. They suggested that re-advances were probably restricted to sites in the southern Andes where precipitation increased during the interval because of the southward shift of the Westerlies. Moreover, sites where the change in climate was insufficient to overcome the main deglaciation trend probably show no record of the event. In contrast, Lumey and Switsur (1993) and Ashworth and Hoganson (1993) do not share this view. Note also that Heusser and Rambassa (1987), Heusser (1989b, 1993) and Clapperton et al. (1989) report an ACR imprint in pollen spectra while Markgraf (1991, 1993) suggests that the observed changes may be a response to local rather than global factors.

This short overview indicates that the onset of a mid-deglaciation cold phase in the Southern Hemisphere is not unequivocally documented. In this context, the slight increase in dust concentration during the ACR revealed in the EPICA ice core is of particular importance for paleoclimatic reconstruction. It is however difficult to attribute this change to one or more specific parameters. This feature does not resemble a return to glacial conditions, but reflects some slight climatic change in the source area at this time.

4.3 Glacial and interglacial dust transport

The size distribution of aeolian dust deposited at remote polar sites is essentially influenced by the dynamics of the atmosphere, such as the wind velocity and distance from the sources (Pye 1987). Moreover, other factors could be important such as the environmental conditions at the source affecting soil and vegetation typologies as well as the efficiency of scavenging by precipitation during transport. Two main questions arise from the profile of EPICA dust distribution parameters. First, what is the cause of the difference between the well-sorted and slightly finer glacial particles and the heterogeneous interglacial particles? Second, what is the reason for the increase in the mode of the particles over the Holocene period?

Our data for EPICA indicates that the mass distribution of dust is centred around a modal diameter of approximately 2 μm with a geometric mean standard deviation of 1.6–1.8 along the core. For old Dome C and Vostok cores, Royer et al. (1983) and De Angelis et al. (1984) obtained values similar to ours for modal diameter, while their σ_g was only slightly higher (2.2 ± 0.2). For Holocene samples, Petit et al. (1981) and De Angelis et al. (1984) suggested a shift toward smaller particles in comparison with LGM samples. In contrast, our results from EPICA indicate an increase toward larger modes. In the light of these new high size-resolution measurements, we believe that the previous data, obtained using a 16 channel counter instead of a 256-channel counter, may be highly inaccurate.

During the LGM period, the parameters of the dust distribution from EPICA are very similar for all samples while those for the Holocene period display a variability between samples. Generally speaking, the LGM distributions have an almost constant mode and the lowest σ_g values. This fact cannot be related to the longer time intervals covered by the LGM samples with respect to the Holocene samples. Averaging consecutive Holocene distributions will lead to a mean distribution with

greater σ_g values. During the Holocene, there is a general gradual increase in the mode and in σ_g. The highest values of the mode are observed in the late Holocene, from about 2 to 7 kyr BP (Fig. 4d).

Figure 5 shows the LGM/Holocene relative and absolute ratios of the fraction of particles in each size interval. This ratio changes with particle size from values greater than 50 (for particles from 0.7 to 3μm) to less than 10 for particle of 5μm. For particles from 2 to 5 μm, the ratio decreases approximately as a function of the third power of the diameter. This means that the LGM size distribution does not represent a simple homothetic amplification of the Holocene distribution and vice versa. Holocene samples display a large-particle enrichment with respect to the LGM. Conversely, LGM show a large-particle depletion, suggesting that gravitational settling has occurred. Therefore, our data suggest that LGM dust remained in the atmosphere longer to allow the settling of large particles. Small-sized particles remain because of their longer residence time. This in turn can be linked to different mechanisms of transport between the two climatic periods.

Significant change in ice core dust-size distribution have been also observed in the Northern Hemisphere for the Penny Ice Cap (Zdnanowicz et al. 2000). The mode was close to 1 μm during the glacial period and at the time of the large Laurentide ice sheet. Then, after deglaciation, the mode shifts to very large particles (up to 6 μm) for the Holocene period because the dust source was closer. For EPICA the change in particle size could be due to the possible contribution of an additional source of dust, absent during the LGM period. This remains possible since to date, the dust sources for the Holocene period are not as well-defined by isotopic finger printing as the LGM dust samples. This is because of technical problems associated with the very low dust content. However, preliminary measurements tend to confirm that the isotopic signature for the Holocene has the same geographical origin, i.e. South America (Basile 1997, and personal communication). So, we believe that the dust source for the Antarctic dust record remained the same (South America) over the entire period.

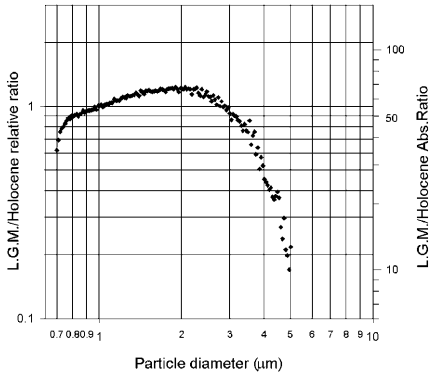

Fig. 5. LGM/Holocene relative and absolute ratios of particles for each size interval (measurement channel). Glacial dust enrichment is greater than 50 for particles with diameters between 1 and 3 μm and decreases steadily for larger particles

We therefore have to consider the change in transport mode. During the glacial period, Antarctica was surrounded by widespread sea-ice cover both in winter and summer (Denton et al. 1991) and the polar front was displaced further north. The strengthening of the polar vortex by the sharp latitudinal thermal gradient may have favoured higher geostrophic winds and well-marked zonal circulation. These conditions caused the interior of the Antarctic East plateau to be more isolated from storm tracks or from the direct penetration of middle latitude air masses. In opposition, during the Holocene period, the drastic reduction of sea ice and the progressive warming of the Southern Ocean weakened the southward polar front allowing air masses and aerosol to penetrate more easily into Antarctica. This suggests that a more effective meridional circulation prevailed.

With such a scenario, longer dust trajectories are expected for the LGM. The continental deflation was intense and the atmospheric dust load for mid-latitudes was likely high. The reduction in the intensity of the hydrological cycle and the decreasing aerosol scavenging efficiency led to a longer residence time in the atmosphere. This may account also for the effective sorting of the particles and the low variability in the size distribution parameters of LGM dust. In opposition, for Holocene dust, sources were weaker, and the reduced residence time of the dust in the atmosphere with a shorter time for transport to Antarctica led to less effective sorting of particle size (i.e. high σ_g) as well as the possibility for larger particles or distributions with high modes to be transported over the Antarctic plateau. This may also account for the higher variability in dust concentration and in particle size parameters.

Such a scenario, linking the glacial/interglacial particle characteristics and mode of transport, seems consistent with the interpretation of Zielinski and Mershon (1997) concerning the dust distribution parameters found in GISP2 Greenland ice. The authors stated that the mass mean diameter of particles could be considered as a proxy for paleo-storminess, while mean number diameter could be related to increased Westerlies intensity that, in turn, is dependent on latitudinal temperature and pressure gradients.

Concerning the gradual increase of the mode of Holocene dust (Fig. 4d, e), several factors may again be involved. One is environmental changes at the source. The first five millennia of the Holocene have been characterised in southern South America by high temperatures, relatively high precipitation and vegetation patterns of the forest-steppe type. The second part of the interglacial instead seems to be cooler and wetter with a diminishing of open vegetation and with woodland converted to closed forest (Heusser 1989b). Paleovegetation data also suggest increased storminess and cloud cover in the second part of the Holocene. These changes

may directly affect the biological activity in soils as well as the pedogenetic processes. This could affect dust particle characteristics by agglomerating or flocculating fine particles. Mineralogical studies of Holocene samples focused on clay minerals, which are mainly derived from physical and chemical rock weathering and represent the final product of soil genesis, would be useful in this matter (Maggi 1997).

4.4 Comparison with the Greenland GRIP dust record

The parameters of the size distribution of dust from different climatic periods in the Greenland GRIP core (Steffensen 1997) are compared with EPICA data in Table 3. The mode of the distribution of GRIP dust fitted by a log normal distribution ranges from 1.5 to 2 μm, which is slightly smaller than for EPICA. No clear trend in mode of distribution is observed between the Glacial and Holocene period and the finest values have been observed for the Pre-Boreal (warm) period. The geometric standard deviation (σ_g) is also in the same range as EPICA values and the lowest values and the best-sorted distributions are also suggested for the LGM period.

In Fig. 6 the dust and isotope profiles of EPICA and GRIP cores are compared for the time interval between 8 and 27 kyr BP. The calcium record is taken as a proxy for continental dust for GRIP (Steffensen 1997), calcium representing mostly the contribution of soluble carbonates from soils in the source areas. Despite the different time resolution, the most significant difference between the two profiles concerns the timing and amplitude of the oscillations. The transitions from cold to mild periods and vice-versa are marked in the Greenland record by very rapid shifts in calcium content (a few decades) that are closely correlated with $\delta^{18}O$ (Fuhrer et al. 1999). This has been attributed mainly to changes in circulation patterns at the highest latitudes of the Northern Hemisphere, coupled with increased dust mobilisation at the Asian source (Fuhrer et al. 1999). On the other hand, the dust oscillations in the EPICA core are less accented and appear to be smoothed. Moreover, dust changes are less correlated with temperature fluctuations than in the GRIP record. The ACR period and the absolute minimum of dust at circa 11.5 kyr BP clearly demonstrate the differences between the dust and temperature signals. This different behaviour has been confirmed by additional dust measurements (not shown) with an enhanced resolution as well as in the non-sea-salt calcium from continuous flow line analysis (Rothlisberger et al. 2000).

During deglaciation, Greenland and EPICA profiles differ significantly. During the warm Bolling phase and through the Alleröd period, dust would appear to have been present at lower levels relative to the glacial stage. At this time, the ACR occurred in Antarctica and dust remained at a substantial level (twice the Holocene value). At the onset of the cold Younger Dryas (12.7 kyr BP), dust rose steadily to glacial levels in Greenland until the end at 11.5 kyr BP, where it drops to the low Holocene value. In contrast, dust decreases in Antarctica from 12.5 kyr BP and this trend continues to the lowest concentration reached at 11.7–11.5 kyr BP. Finally, EPICA and Greenland records both display low dust content at 11.5 kyr BP, corresponding to a steady warming in both records as well as a wet period probably of global extent.

5 Conclusions

The new set of measurements of the concentration and size distribution of insoluble microparticles obtained using a high-resolution counter has made it possible to document the LGM/Holocene period spanning the last 27000 years. The EPICA dust record introduces new considerations on the dynamics of the past climate in the Southern Hemisphere. During the last glacial period, the

Table 3. Comparison between lognormal fit parameters from selected samples representing different climatic periods in EPICA (a) and GRIP (b, from Steffensen 1997) ice cores

EPICA	Lognormal modal Diameter (Dv)	σg	Number of samples averaged	Time interval (yr BP)
[a]				
Holocene	2.06 ± 0.21	1.80 ± 0.10	70	2400–11300
ACR	1.94 ± 0.17	1.73 ± 0.09	19	11900–14300
Deglaciation	1.79 ± 0.11	1.65 ± 0.06	25	14700–19200
LGM	1.91 ± 0.02	1.60 ± 0.01	30	20000–27000
GRIP	Lognormal modal Diameter (Dv)	σg	Number of samples	Time interval (yr BP)
[b]				
Holocene	1.60–1.80	1.71	350	(32–2023)–(3029–3045)
Pre-Boreal	1.50	1.74	75	10181–11450
Younger Dryas	1.68	1.57	49	11612–11714
Bølling	1.54	1.75	99	14320–14410
Pre-Bølling	1.66	1.71	21	14493–14601
Glacial	1.76	1.65	66	15839–16362
LGM	1.94–2.02	1.61-1.68	154	21644–22143

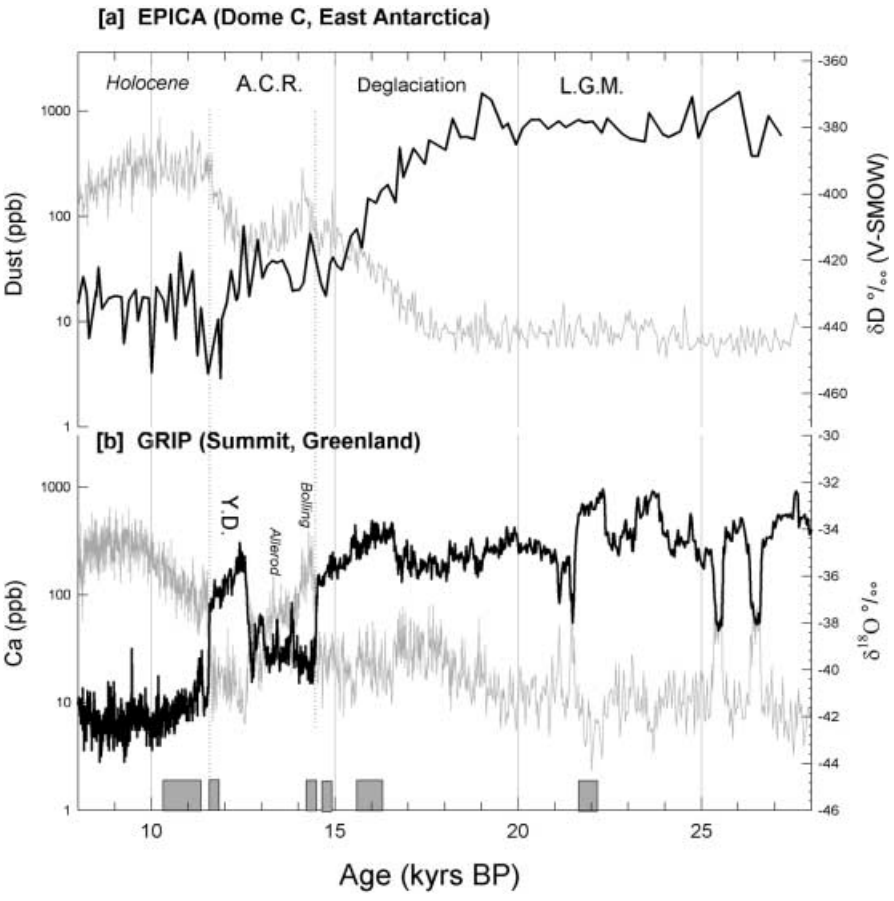

Fig. 6. a, b Dust (*black line*) and isotope (*grey line*) records of EPICA ice core, Calcium (*black line*) and isotope (*grey line*) records for GRIP ice core from 8 to 28 kyr BP. The *grey areas* at the *bottom* represent the climatic interval investigated for insoluble particle distribution characterisation by Steffensen (1997) and shown in Table 3b

dust flux in East Antarctica was 26 times the Holocene level, an increase which is slightly higher than the previous estimate. For the ACR, a slight but significant dust concentration has been observed for the first time in Antarctica, indicating a substantial depression of climate and environment in South America during the same period, but not synchronous with the Younger Dryas. Also, a well-marked minimum in dust concentration occurred at 11.5–11.7 kyr that corresponds to the steady warming which immediately followed the end of the cold phase of the Younger Dryas in the Northern Hemisphere. This minimum dust concentration is interpreted as corresponding to a wet period. Indeed such a wet period, probably associated with a milder climate, would not have been restricted to the Northern Hemisphere and may have strongly affected the source region for dust in Antarctica.

The parameters of the size distribution of the particles indicate that the mode of dust for the LGM is smaller and the particles better sorted than for dust deposited during the warm Holocene period. We suggest that different long-range transport modes are involved for the continental dust. During the glacial period, a combination of factors such as sea-ice extension and the northward shift of the polar front formed a more efficient barrier to the penetration of air masses into Antarctica. In spite of the increase of the polar vortex and zonal circulation, dust particles remained longer in the atmosphere thanks to a lower efficiency of dust scavenging by precipitation. This is in contrast to the Holocene pattern for which the penetration of air masses in Antarctica is likely easier and atmospheric circulation more meridional. The drastic change in the environment of the dust source (likely southern South America) as well as the reduced residence time of particles related to an enhanced hydrologic cycle, steadily contributed to the reduction in the dust transported to Antarctica.

Comparison of EPICA and Greenland dust records shows significant differences in timing and magnitude. The rapid dust changes observed in the Greenland core are sharp and closely correlated to temperature variations. In Antarctica, this relation is not as direct as is demonstrated by the modest increase of dust during the cold phase of the ACR.

Finally, the Holocene part of the record shows a general decrease of aerosol concentration that could suggest a gradual reduction of primary production and/or mobilisation of dust at the source. The distribution parameters show higher modes with the highest values in the second part, possibly reflecting a gradual change at the source such as the evolution of soil characteristics.

Acknowledgements This is EPICA publication 22. This work is a contribution to the "European Project for Ice Coring in Antarctica" (EPICA), a joint ESF (European Science Foundation)/EC

scientific programme, funded by the European Commission under the Environmental and Climate Programme (1994–1998) contract ENV4-CT95–0074 and by national contributions from Belgium, Denmark, France, Germany, Italy, the Netherlands, Norway, Sweden, Switzerland and the United Kingdom. We thank the reviewers for their comments and suggestions allowing us to improve the manuscript.

References

Ashworth AC, Hoganson J (1993) The magnitude and rapidity of the climate change marking the end of the Pleistocene in the mid-latitudes of South America. Palaeogeogr Palaeoclimatol Palaeoecol 101: 263–270

Basile I (1997) Origine des arosols volcaniques et continentaux de la carotte de glace de Vostok (Antarctique). PhD Thesis, LGGE-Universit Joseph Fourier – Grenoble I Grenoble, 254 p

Basile I, Grousset FE, Revel M, Petit JR, Biscaye PE, Barkov NI (1997) Patagonian origin of glacial dust deposited in East Antarctica (Vostok and Dome C) during glacial stages 2, 4 and 6. Earth Planet Sci Lett 146: 573–589

Basile I, Petit JR, Touron S, Grousset FE, Barkov NI (2001) Volcanic tephra in Antarctic (Vostok) ice-cores: source identification and atmospheric implications. J Geophys Res, 106 D23, 31915–931

Briat M, Royer A, Petit JR, Lorius C (1982) Late glacial input of eolian continental dust in the Dome C ice core: additional evidence from individual microparticle analysis. Ann Glaciol. 3: 27–30

Burckle LH, Cooke DW (1983) Late Pleistocene Eucampia antarctica abundance stratigraphy in the Atlantic sector of the Southern Ocean. Micropaleontology 29: 6–10

Burkle LH, Cirilli J (1987) Origin of Diatom ooze belt in the Southern Ocean: implications for late Quaternary paleoceanography. Micropaleontology 33: 86

Chappellaz JA, Blunier T, Reynaud D, Barnola JM, Schwand J, Stauffer B (1993) Synchronous changes in atmospheric CH4 and Greenland climate between 40 and 8 kyr BP Nature 366: 443–445

Charles CD, Fairbanks RG (1992) Evidence from Southern Ocean sediments for the effect of North Atlantic deep-water flux on climate. Nature 355: 416–419

Clapperton CM (1993) Nature of environmental changes in South America at the Last Glacial Maximum Palaeogeogr Palaeoclimatol Palaeoecol 101: 189–208

Clapperton CM, Sugden DE, Birnie J, Wilson M (1989) Late-glacial and Holocene glacier fluctuations and environmental change in South Georgia, southern ocean. Quat Res 31: 210–228

Clapperton CM, Sugden DE, Kaufman DS, McCulloch R (1995) The last glaciation in the central Magellan strait, southernmost Chile. Quat Res 44: 133–148

COHMAP Project Members (1988) Climatic changes of the last 18000 years: observations and model simulations. Science 241: 1043–1052

De Angelis M, Legrand M, Petit JR, Barkov NI, Korotkevitch YS, Kotlyakov VM (1984) Soluble and insoluble impurities along the 950 m deep Vostok ice core (Antarctica) – climatic implications. Journal of Atmospheric chemistry 1: 215–239

De Angelis M, Barkov NI, Petrov VN (1987) Aerosol concentrations over the last climatic cycle (160 kyr) from an Antarctic ice core. Nature 325: 318–321

De Baar HJW, Jong JTMD, Bakker DCE, Loscher BM, Veth C, Bathmann U, Smetacek V (1995) Importance of iron for plankton blooms and carbon dioxide drawdown in the Southern Ocean. Nature 373: 412–415

Denton GH, Prentice ML, Burkle LH (1991) Cainozoic history of the Antarctic ice sheet. In: Tingey RJ (ed) Geology of Antarctica, 17. Oxford Science Publications, Oxford, 44, pp.363–433

Denton GH, Heusser CJ, Lowell TV, Moreno PI, Andersen BG, Heusser LE, Schluchter C, Marchant DR (1999) Interhemispheric linkage of paleoclimate during the Last Glaciation. Geografisk Ann 81A(2): 107–153

Fairbanks RG (1989) A 17,000-year glacio-eustatic sea level record: influence of glacial melting rates on the Younger Dryas event and deep-ocean circulation. Nature 342: 637–642

Fuhrer K, Wolff EW, Johnsen SJ (1999) Timescales for dust variability in the Greenland Ice Core Project (GRIP) ice core in the last 100000 years. Geophys Res 104: 31043–31052

Gaudichet A, Petit JR, Lefevre R, Lorius C (1986) An investigation by analytical transmission electron microscopy of individual insoluble microparticles from Antarctic (Dome C) ice core samples. Tellus 38B: 250–261

Gaudichet A, De Angelis M, Lefevre R, Petit JR, Korotkevitch YS, Petrov VN (1988) Mineralogy of insoluble particles in the Vostok Antarctic ice core over the last climatic cycle (150 Kyr). Geophys Res Lett 15: 1471–1474

Gaudichet A, De Angelis M, Joussaume S, Petit JR, Korotkevitch YS, Petrov VN (1992) Comments on the origin of dust in East Antarctica for present and ice age conditions. Atmos Chem 14: 129–142

Grousset FE, Biscaye PE, Revel M, Petit JR, Pye K, Joussaume S, Jouzel J (1992) Antarctic (Dome C) ice-core dust at 18 ky BP: isotopic constraints and origins. Earth Planet Sci Lett 111: 175–182

Hansson ME (1994) The Renland ice core. A Northern Hemisphere record of aerosol composition over 120000 years. Tellus 46B: 390–418

Heusser CJ, Rambassa J (1987) Cold climatic episode of Younger Dryas age in Tierra del Fuego. Nature 328: 609–611

Heusser C (1989a) Polar perspective of Late-Quaternary climates in the Southern Hemisphere. Quat Res 32: 60–71

Heusser CJ (1989b) Late quaternary vegetation and climate of southern Tierra del Fuego. Quat Res 31: 396–406

Heusser CJ (1993) Late-Glacial of Southern South America. Quat Sci Rev 12: 345–350

Hulton N, Sugden D, Payne A, Clapperton C (1994) Glacier modeling and the climate of Patagonia during the last glacial maximum. Quat Res 42: 1–19

Joussaume S (1989) Desert dust and climate: an investigation using an atmospheric general circulation model. In: Leinen M, Sarnthein M (eds) Paleoclimatology and paleometeorology: modern and past patterns of global atmospheric transport. NATO Workshop, pp 253–263

Joussaume S (1990) Three-dimensional simulation of the atmospheric cycle of desert dust particles using a general circulation model. Geophys Res 95: 1909–1941

Jouzel J, Lorius C, Petit JR, Genthon C, Barkov NI, Kotlyakov VM, Petrov VM (1987) A continuous isotope temperature record over the last climatic cycle (160000 years). Nature 329: 403–408

Jouzel J, Vaikmae R, Petit JR, Martin M, Duclos Y, Stievenard M, Lorius C, Toots M, Melires MA, Burckle LH, Barkov NI, Kotlyakov VM (1995) The two-step shape and timing of the last deglaciation in Antarctica. Clim Dyn 11: 151–161

Jouzel J, Masson V, Cattani O, Falourd S, Stievenard M, Stenni B, Longinelli A, Johnsen SJ, Steffensen JP, Petit JR, Schwander J, Souchez R (2001) A new 27 ky high resolution East Antarctic climate record. Geophys. Res. Lett 28, 16, 3199–3202

Kukla G (1989) Long continental records of climate–an introduction. Palaeogeogr Palaeoclimatol Palaeoecol 72: 1–9

Kumar N, Anderson RF, Mortlock RA, Froelich PN, Kubik P, Ditrich-Hannen B, Suter M (1995) Increased biological productivity and export production in the glacial Southern Ocean. Nature 378: 675–680

Lamy F, Hebbeln D, Wefer G (1999) High-resolution marine record of climatic change in mid-latitude Chile during the last 28000 years based on terrigenous sediment parameters. Quat Res 51: 83–93

Lumey SH, Switsur R (1993) Late Quaternary chronology of the Titao Peninsula, southern Chile. J Quat Sci 8 : 161–165

Maggi V (1997) Mineralogy of atmospheric microparticles deposited along the GRIP ice core. Geophys Res 102: 26725–26734
Mahowald N, Kohfeld K, Hansson M, Balkanski Y, Harrison SP, Prentice IC, Schulz M, Rodhe H (1999) Dust sources and deposition during the Last Glacial Maximum and current climate: a comparison of model results with paleodata from ice cores and marine sediments. Geophys Res 104: 15895–15916
Marden CJ, Clapperton CM (1995) Fluctuations of the South Patagonia Icefield during the last glaciation and the Holocene. J Quat Sci 10: 197–210
Markgraf V (1991) Younger Dryas in South America? Boreas 20: 63–69
Markgraf V (1993) Younger Dryas in southernmost South America – an update. Quat Sci Rev 12: 351–355
McCulloch RD, Bentley MJ (1998) Late glacial advances in the strait of Magellan, southern Chile. Quat Sci Rev 17: 775–787
McCulloch RD, Bentley MJ, Purves RS, Hulton NRJ, Sugden DE, Clapperton CM (2000) Climatic inferences from glacial and palaeoecological evidence at the last glacial termination, southern South America. J Quat Sci 15: 407–417
Patterson EM, Gillette DA (1977) Commonalities in measured size distribution for aerosol having a soil-derived component. Geophys Res 82: 2074–2082
Petit JR, Briat M, Royer A (1981) Ice Age aerosol content from East Antarctic ice core samples and past wind strength. Nature 293: 391–394
Petit JR, Mounier L, Jouzel J, Korotkevich YS (1990) Paleoclimatological and chronological implications of the Vostok core dust record. Nature 343: 56–58
Petit JR, Jouzel J, Raynaud D, Barkov NI, Barnola JM, Basile I, Bender M, Chappellaz J, Davis M, Delaygue G, Delmotte M, Kotlyakov VM, Legrand M, Lipenkov VY, Lorius C, Ppin L, Ritz C, Saltzman E, Stievenard M (1999) Climate and atmospheric history of the past 420000 years from the Vostok ice core, Antarctica. Nature 399: 429–436
Pye K (1987) Aeolian dust and dust deposits. Academic Press, San Diego, pp 334
Rea DK (1994) The paleoclimatic record provided by eolian deposition in the deep sea: the geologic history of wind. Rev Geophys 32: 159–195
Rothlisberger R, Hutterli MA, Sommer S, Wolff EW, Mulvaney R (2000) Factors controlling nitrate in ice cores: evidence from the Dome C deep ice core. J Geophys Res 105 (D16): 20565–20572
Royer A, De Angelis M, Petit JR (1983) A 30000 year record of physical and optical properties of microparticles from an East Antarctic ice core and implications for paleoclimate reconstruction models. Clim Change 5: 381–412
Schwander J, Jouzel J, Hammer CU, Petit JR, Udisti R, Wolff E (2001) A tentative chronology for the EPICA Dome Concordia ice core. Geophys Res Lett 28, 22, 4243–4246
Simmonds I (1981) The effect of sea ice on a general circulation model of the Southern Hemisphere. Int Ass Hydrol Sci Publ 131: 193–206
Sokolik IN, Toon OB (1996) Direct radiative forcing by anthropogenic airborne mineral aerosols. Nature 381: 681–683
Steffensen JP (1997) The size distribution of microparticles from selected segments of the GRIP ice core representing different climatic periods. J Geophys Res 102 (C12): 26755–26763
Svensson A (1998) Characterization of continental dust in the Greenland GRIP ice core back to 44 kyr BP. PhD Thesis, University of Copenhagen, Denmark, pp 84
Thompson LG, Mosley-Thompson E, Davis ME, Lin PN, Henderson KA, Cole-Dai J, Bolzan JF, Liu KB (1995) Late glacial stage and Holocene tropical ice core records from Huascarn, Peru. Science 269: 46–50
Wenzens G (1999) Fluctuations of outlet and valley glaciers in the Southern Andes (Argentina) during the Past 13000 years. Quat Res 51: 238–247
Yung YL, Lee T, Wang CH, Shieh YT (1996) Dust: a diagnostic of the hydrologic cycle during the Last Glacial Maximum. Science 271: 962–963
Zielinski GA, Mershon GR (1997) Paleoenvironmental implications of the insoluble microparticle record in the GISP2 (Greenland) ice core during the rapidly changing climate of the Pleistocene-Holocene transition. Geol Soc Am Bull 109: 547–559
Zdanowicz CM, Zielinski GA, Wake CP, Fisher DA, Koerner RM (2000) A Holocene record of atmospheric dust deposition on the Penny Ice Cap, Baffin Island, Canada. Quat Res 53: 62–69